Book chapter in: 'Planar Lipid Bilayers (BLMs) and their Applications'.
H.T. Tien und A. Ottova-Leitmannova (Editors). Elsevier, Amsterdam. 2003. pp. 269-293

Chapter 8

Coupling of chain melting and bilayer structure: domains, rafts, elasticity and fusion

T.Heimburg

Membrane Biophysics and Thermodynamics Group,
Max-Planck-Institute for Biophysical Chemistry, 37077 Göttingen, Germany

1. INTRODUCTION

Lipid membranes in biology have a complex composition, consisting of hundreds of different lipids and proteins, plus various steroids like cholesterol. Therefore extensive research on the physical and physico-chemical properties of lipids took place in the 1970s and 1980s [1, 2]. However, the interest in lipids somewhat declined among biochemists, because at the time there was no obvious connection between the physical properties of the model systems and biological membranes. At the same time, the emphasis shifted to the development of single molecule recording methods (e.g. patch clamp [3]), which strengthened the belief in the predominant relevance of single proteins for biological function [4]. Textbooks

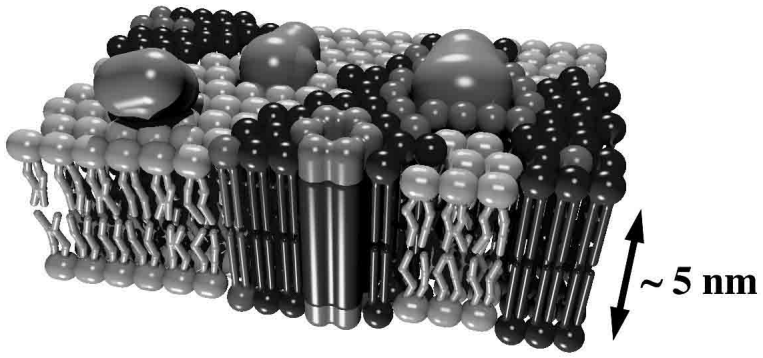

Figure 1: Schematic drawing of a biological membrane, showing lipids of different nature and state distributed inhomogeneously within the membrane plane. Proteins penetrate through the membrane or are bound to its surface.

of Biochemistry and Physiology [5] focus on reactions on the single molecular level, for example on ion conductance of single channel proteins as the potassium channel. The lipid membrane is considered by many scientists as the supporting matrix for the proteins, and no independent role is attributed to it. In this contribution we challenge this view. Many properties of surfaces cannot be understood on a single molecule level, for example the the lateral distribution of molecules, and physical features such as elastic constants, curvature, and fusion and fission events of vesicles.

The lipid composition is known to vary between different organelles within one cell. Mitochondria display a high fraction of charged lipids (mainly cardiolipin) and hardly any sphingolipids, whereas plasma membranes are rich in cholesterol and sphingolipids [6]. Nerve membranes, on the other hand, are rich in lipids with polyunsaturated fatty acid chains. The lipid composition of bacterial membranes depends on their growth temperature [7]. The reason for the large diversity in membrane composition is largely unknown.

Bilayers composed of a single lipid species display an order-disorder transition (the so-called melting transition) in a temperature regime, which is of biological relevance in a broader sense. This means that membranes consisting of extracted biological lipids have melting points close or not too far away from physiological temperature (-20° to +60° C). The low temperature lipid state has hydrocarbon chains predominantly ordered in an all-trans configuration and is for historical reasons called the ‘gel’ state. The high temperature state with unordered chains is called the ‘fluid’ state. Unsaturated lipids (containing double bonds in the hydrocarbon chains) display significantly lower melting temperatures as saturated lipids. Distearoyl phosphatidylcholine (DSPC) is a saturated lipid with 18 carbons per hydrocarbon chain, displaying a melting transition at about 55°C. Dioleoyl phosphatidylcholine (DOPC) is identical to DSPC except for one double bond in the center of each hydrocarbon chain. This small change in chemical structure leads to a lowering of the melting point to about -20°C. Since a large fraction of the lipids of biological membranes are unsaturated, there is a common but unjustified belief that melting transitions in biological membranes occur below the physiological temperature regime.

We will now outline why this is incorrect in our opinion. Fig. 2 shows heat capacity profile of different artificial and biological membranes. Fig. 2a is the melting of dipalmitoyl phosphatidylcholine (DPPC) multilamellar membranes, a lipid system that forms spontaneously upon dissolving the dry lipid in water. This system displays a highly cooperative melting peak at 41°C with a half width of about 0.05 K. A fine detail in this melting profile is the so called pretransition (see insert) which will play a role in section 5, but will not be considered here in more detail. Fig. 2b displays an equimolar mixture of two lipids, dimyristoyl phosphatidylcholine (DMPC) and distearoyl phosphatidylcholine (DSPC).

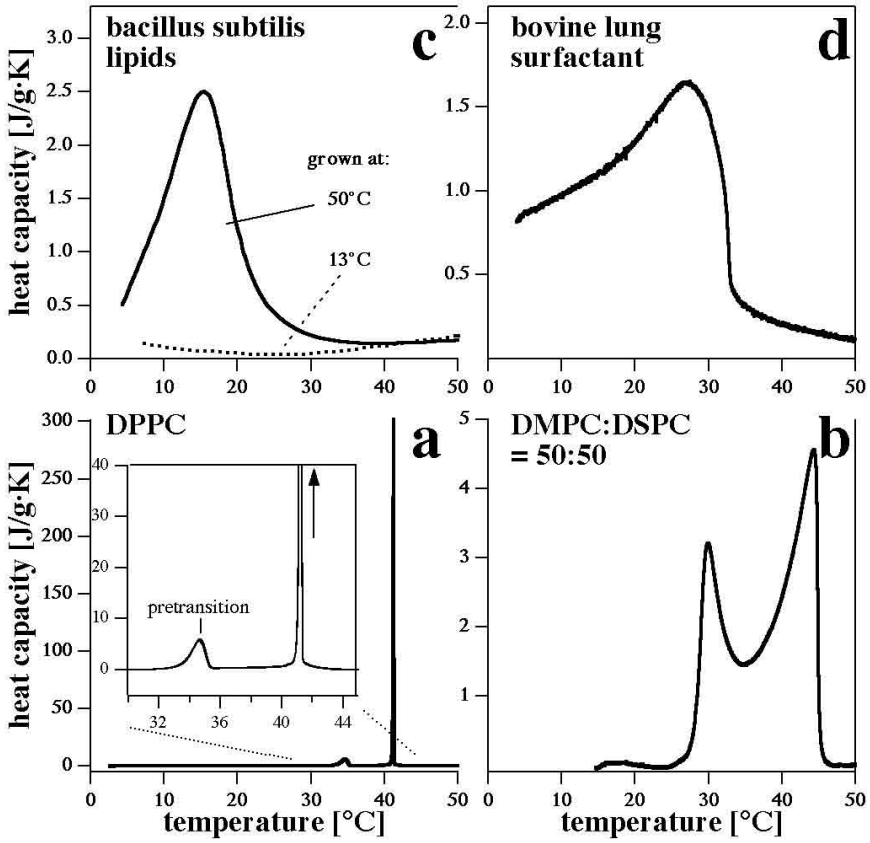

Figure 2: Melting profiles of different artificial and biological samples: a. Dipalmitoyl phosphatidylcholine (DPPC) multilamellar vesicles. The insert is a magnification which shows the pretransition in more detail. b. Dimyristoyl phosphatidylcholine(DMPC):distearoyl phosphatidylcholine(DSPC) equimolar mixture. c. Lipid extract from bacillus subtilis cells grown at 50°C and at 13°C (adapted from [7]). d. bovine lung surfactant [8].

DMPC alone melts at 24°C, whereas DSPC melts at 55°C. The melting profile of the mixture, however, displays a continuous melting event between 27°C and 46°C. Thus, the melting transition of a mixture is not just a cooperative melting at a temperature which represents the arithmetic mean of these temperatures (which for this mixture is about 39°C), but is rather represented by an extended temperature regime. This behavior can be understood by simple theoretical concepts such as regular solution theory, which is based on the macroscopic separation of gel and fluid domains in the melting regime [9]. Now regular solution theory is very useful for the understanding of the principles of phase diagrams, but is not accurate enough to explain details about the distribution of molecules. Mixtures of many components - as in biological membranes - can result in very broad melting profiles. The absence of a pronounced melting peak, found in many biological systems in no way means that there are no melting events. The chain melting, for example, may be so spread out over a large temperature regime that it becomes difficult to distinguish it from the base line.

The melting profile given in Fig. 2b was analyzed In more detail by Sugar and coworkers [10] using Monte Carlo simulations. In these simulations one can obtain snapshots of the distribution of lipids in the two-dimensional plane as a function of temperature. Seven representative snapshots, calculated at different temperatures, are displayed in Fig. 3. They show that the cause for the continuous nature of the melting is the lateral separation of lipids of different state and nature into nanoscopic, mesoscopic and macroscopic domains. Domains have also been found recently in biological membranes, where they are often called 'rafts' [11, 12, 13, 14, 15]. Rafts are domains, usually rich in sphingolipids and cholesterol, but also in certain proteins. The finding of these structures has refueled the interest in the lipids of biological membranes. In human erythrocytes sphingomyelin has to a very high percentage saturated chain and a high number of carbons (C24) [6]. Cholesterol is known to even further immobilize chain mobility [16] in the quantities found in these membranes (about 20%). Thus, rafts consist of lipids that have high melting points. The finding of rafts is itself a proof for the heterogeneous nature of biological membranes.

We will now discuss the melting profiles of biological samples. Fig. 2c displays

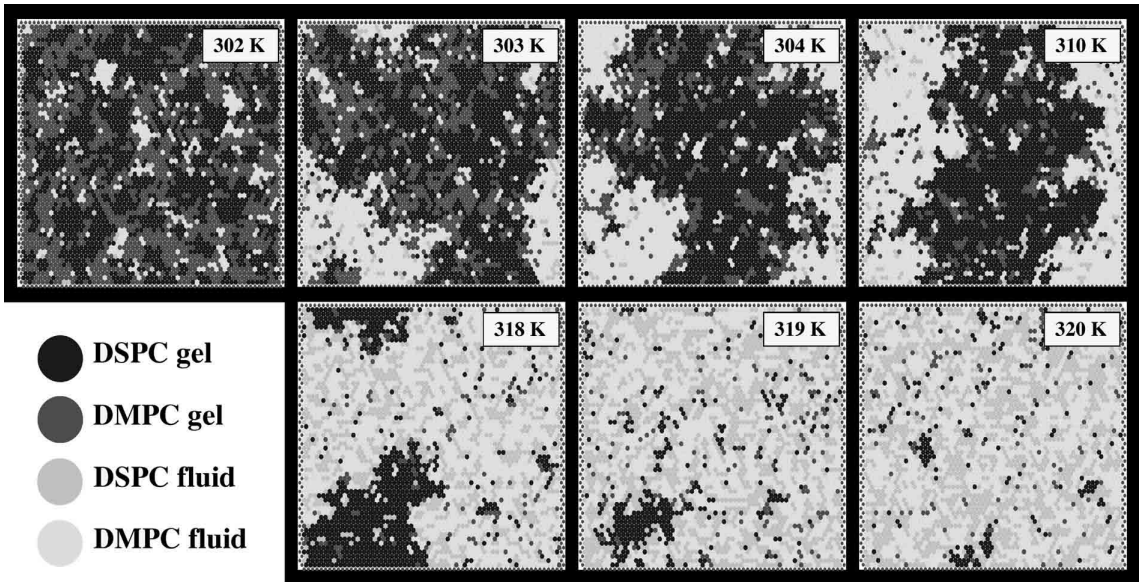

Figure 3: Series of snapshots from a computer simulation of the melting process of DMPC:DSPC=50:50 mixtures shown in Fig. 2b at various temperatures. Given in four different grey shades are gel state lipids of DSPC and DMPC, and fluid state lipids of DSPC and DMPC, respectively. The progress of domain formation on different length scales and the macroscopic demixing into fluid and gel domains at 310 K can clearly be seen.

the melting of a lipid extract from Bacillus subtilis [7], grown at two different temperatures. The lipids of the population grown at 50°C show a pronounced but broad melting peak at about 15°C which extends to much higher temperatures. The lipids of the same cells grown at 13°C display no obvious melting anomaly,

indicating that the lipid composition in this population is different and the cells felt a need to adjust their lipid composition differently from the population grown at higher temperatures. Van de Vossenberg and coworkers pointed out that this change in physical properties is mainly due to the change in iso-branched and antiso-branched fatty acid chains within the lipids.
Lung surfactant (Fig. 2d) forms a film on the lung surface and prevents it from collapsing. It contains several proteins, known as the surfactant proteins A, B and C (the sample in Fig. 1d had been washed to remove soluble proteins). Lung surfactant displays a pronounced but broad melting peak at 26°C. The upper end of this transition extends to physiological temperature. There are therefore cases where melting events in biological membranes can clearly be shown. However, as pointed out above, mixtures of many components can result in very broad melting profiles, which may be difficult to distinguish from the base line.

We can now pose the following question: Why may nature bother to adjust its lipid composition to environmental conditions?

2. CHAIN MELTING AND FLUCTUATIONS

2.1 Fluctuations in the state of the system

During the melting transition several membrane properties change. The enthalpy increases by about 20-40 kJ/mol, depending on lipid chain length. The volume increases by about 4% and the area by about 25%. Fig. 4 shows the fraction of fluid lipids for dipalmitoyl phosphatidylcholine (DPPC) unilamellar vesicles at the melting point (41°C, obtained in a computer simulation [17, 18]. Although the mean fraction of fluid lipids is, as expected, 50%, at any given time this fraction deviates from the mean. The deviations from the mean value are called fluctuations. During the melting process the fluctuations are strong. At the melting temperature the Gibbs free energies of the fluid and the gel state of a lipid are equal. This implies that it costs no free energy to shift the system from gel to fluid. Therefore, thermal fluctuations are sufficient to induce large alterations in the state of the membrane. The number of gel and fluid state domains will vary in time and between different vesicles, meaning that there are space and time dependent fluctuations in the enthalpy, the volume and the area of the membrane.
The 'fluctuations-dissipation' theorem relates the fluctuations in enthalpy (closely related to the fluctuations in the number of fluid lipids) to the heat capacity:

$$c_P = \frac{\overline{H^2} - \overline{H}^2}{RT^2} \tag{1}$$

Thus, the mean square deviation of the distribution shown in Fig.4 is proportional

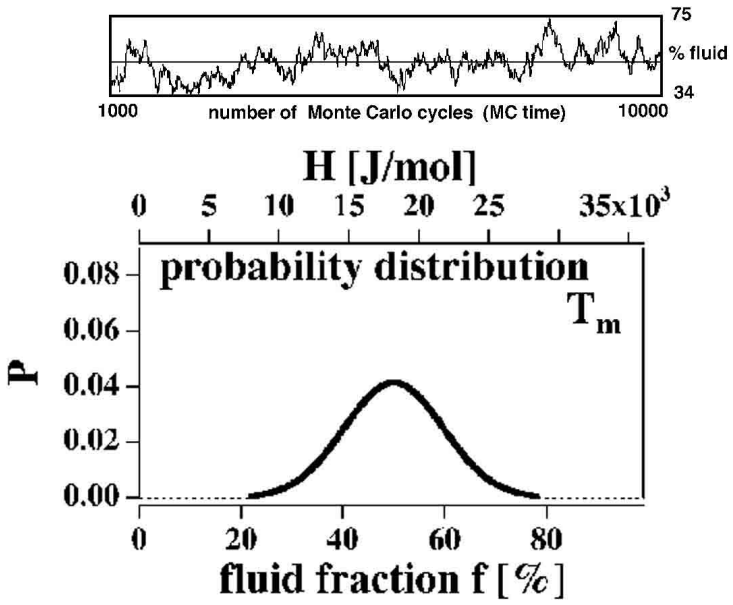

Figure 4: Top: At the melting point of a single lipid membrane, the number of fluid lipids (and its enthalpy) fluctuates around a mean value (50% fluid). Bottom: The distribution of states derived from these fluctuations is roughly given by a Gaussian profile (fat line). The half width of this distribution is related to the heat capacity. Data are taken from computer simulations of the melting profile of DPPC unilamellar vesicles at the melting point [18].

to the heat capacity. This is used in Monte Carlo simulations to derive the heat capacity from the noise produced in the simulation of the enthalpy of a system.

2.2 Fluctuations in composition: Domains and rafts

During a Monte Carlo simulation both the percentage of fluid lipids and the domain sizes fluctuate around a mean value. Since with time lipids undergo a Brownian motion laterally within the membrane, the composition is also subject to fluctuations. The Monte Carlo snapshots shown in Fig. 3 clearly show that depending on temperature domains of different size and composition form. The lateral distribution of molecules has mainly been analyzed by computer simulations making use of experimental heat capacity profiles. Mouritsen and his group working in Denmark have contributed considerably to this understanding of the thermodynamics of lipid mixing [19, 20]. Domain formation is shown to be a function of the physico-chemical properties of the components, and it is strongly influenced by the presence of proteins. Another biomolecule of large importance is cholesterol which is very abundant in biological membranes (up to 30% of the lipid). The general influence of cholesterol on heat capacity profiles is a broadening and shift to higher temperatures. This has been used to construct phase diagrams of lipid bilayers containing cholesterol [16, 21, 20, 20, 22], leading to a

new terminology for lipid phases.
The terms ‘gel’ and ‘fluid’ phase are somewhat misleading, since they do not specify what kind of order is changing. In physics the loss of lateral order (from crystalline to random) is called the solid-liquid transition. Lipids, however, also possess internal degrees of freedom, which may change from an all-trans chain conformation (ordered) to a random chain arrangement (disordered) via trans-gauche isomerizations. Thus, the phases in the lipid-cholesterol diagram can be referred to as solid-ordered (all-trans chains arranged on a crystalline lattice), liquid-ordered (all-trans chains in an unordered or glass-like lateral arrangement) or liquid-disordered (random chains with random lateral arrangement). The first phase resembles the ‘gel’-phase, whereas the latter phase represents the ‘fluid’ phase [22].
The terminology of lipid-cholesterol phase diagrams is now also used to charac-

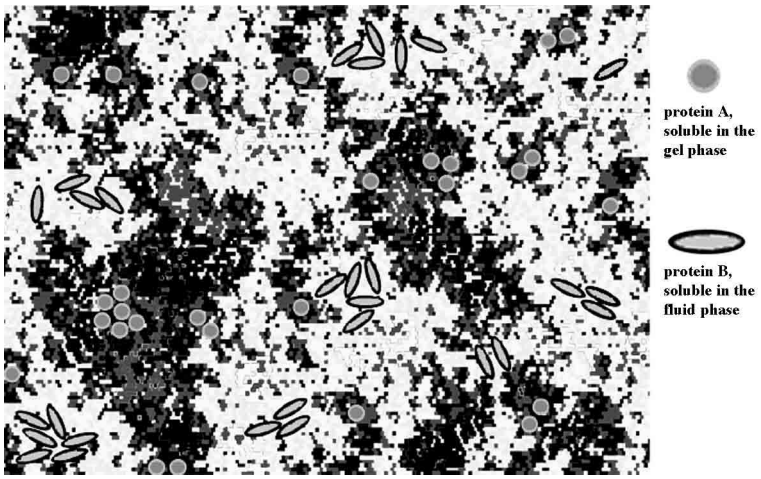

Figure 5: Fig.5. Schematic drawing of a membrane consisting of two lipids in the gel-fluid coexistence regime. Two different kinds of proteins (A and B) are designed to be better soluble in either gel or fluid phase. Thus, these two proteins do not interact in the gel-fluid coexistence regime.

terize certain domain types called rafts which are found in biological membranes. Originally rafts were identified by washing cell membranes in detergent. A certain detergent resistant fraction of the membranes (‘rafts’), was found to be rich in sphingolipids, cholesterol and certain proteins. This was characterized in terms of islands of ordered lipid surrounded by a fluid matrix [11, 12, 14, 13, 15]. There is an ongoing debate between biochemists and physical chemists on whether these rafts are rigid structures or whether they are domains subject to fluctuations in physical state and composition. The author of this article favors the latter view, as he believes that nature in general tries to avoid stable structures. Fluctuating systems change as a response to changes in temperature, pH, and ionic strength, as well to the changes in membrane composition as induced by the binding of proteins or the action of phospholipases. This provides control mechanisms for

nature to adjust to changes in environmental conditions.
It is quite clear that the lateral segregation of membrane components into domains will have a major impact on biological function, because it can influence reaction cascades. A two component lipid matrix in the gel-fluid coexistence regime is shown in Fig. 5. Two proteins are imbedded into the lipid matrix, one with a preference for the gel and the other one with a preference for the fluid phase. Assume furthermore that for biological activity these two proteins have to interact with each other. It is obvious that in the setting of Fig. 5 proteins A and B would not interact with each other because they are located in different domains. Thus, biological activity would be low. Everything that alters the domain arrangement thus changes the function of the membrane. This represents a major control mechanism of a membrane, which is based on the physics of the membrane ensemble rather than on single molecular properties. This feature of a membrane has been overlooked in recent decades and it is exciting to see the recent development of an understanding for the macroscopic control mechanisms of membranes.

2.3. Fluctuations in volume

An important observation is that for most lipid systems the change in volume and enthalpy during the melting transition is exactly proportional [23, 8]. The volume expansion coefficient (dV/dT) and the heat capacity (dH/dT) of a lipid sample are shown in Fig. 6. These two functions are exactly superimposable within experimental error. This has also been demonstrated for other artificial and biological lipid samples [8]. Thus

$$\frac{d\Delta V}{dT} = \gamma \, \frac{d\Delta H}{dT} \qquad \longrightarrow \qquad \Delta V(T) = \gamma \, \Delta H(T) \tag{2}$$

with $\gamma = 7.8 \cdot 10^{-4} cm^3/J$. Therefore, the fluctuations in enthalpy must be related to the fluctuations in volume in a proportional manner.

3. THE ELASTIC CONSTANTS AND RELAXATION TIMES

3.1. Volume compressibility

The fluctuation theorem can also be used to derive an expression for the isothermal volume compressibility:

$$\kappa_T = \frac{\overline{V^2} - \overline{V}^2}{V \cdot RT} \tag{3}$$

Similarly, the area compressibility of a membrane is given by

$$\kappa_T^{area} = \frac{\overline{A^2} - \overline{A}^2}{A \cdot RT} \tag{4}$$

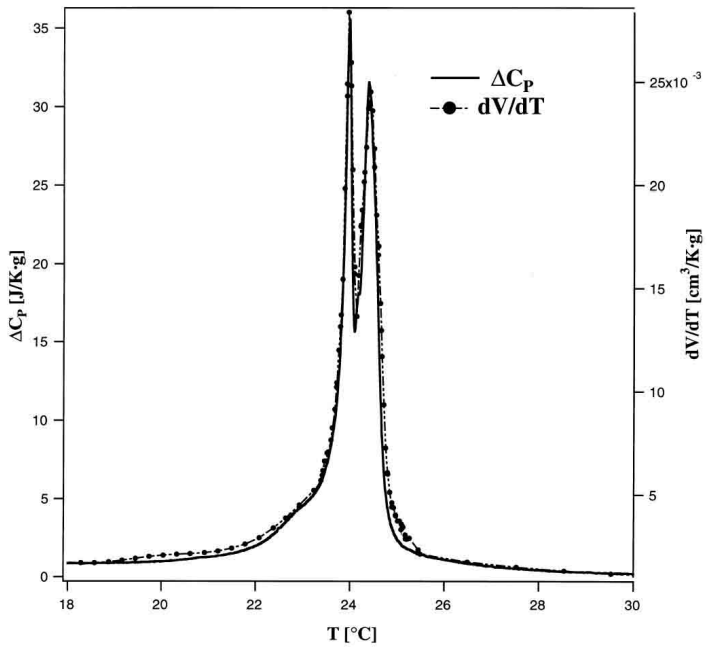

Figure 6: Heat capacity (solid line) and volume expansion coefficient (symbols) of DMPC large unilamellar vesicles (from extrusion). Both functions display identical temperature dependence.

Since enthalpy and volume are proportional to each other, it follows from Eqs. 2 and 3 that

$$\Delta\kappa_T = \frac{\gamma^2 \cdot T}{V} \Delta c_P \qquad , \tag{5}$$

meaning that the change of the isothermal volume compressibility in the melting regime is proportional to the heat capacity. In other words, the compressibility is high in the melting regime. If the heat capacity is given in molar units, the volume V is the volume per mol of lipid. Interestingly, the constant γ was found to be the same for all lipids, even in a biological sample such as lung surfactant ($\gamma = 7.8 \cdot 10^{-4} cm^3/J.$). Eq.5 was shown to be correct from ultrasonic experiments [24, 25].

3.2. Area compressibility and bending elasticity

A proportional relation can also be assumed between area changes and enthalpy of the membrane. This relation is much more difficult to measure and therefore

it was first used as a postulate [23]. If this were the case, one would also obtain a proportional relation between area compressibility changes and excess heat capacity:

$$\Delta\kappa_T^{area} = \frac{\gamma_{area}^2 \cdot T}{A}\,\Delta c_P \qquad . \tag{6}$$

From crystallographic and NMR data it has been deduced that the total area change in the transition is about 25%. It can also be concluded from these data that the γ_{area} is approximately $9 \cdot 10^3 cm^2/J$. If the heat capacity is given in molar units, the area A is the area per mol of lipid. Eq. 6 is important for the determination of the curvature elasticity of membranes. Evans [26] derived an expression for the bending rigidity of membranes, based on the simplifying assumption that bending requires lateral expansion of the outer monolayer and compression of the inner monolayer. Using his derivations, simple relations can also be obtained for the bending elasticity (or the bending modulus, respectively). For a symmetric homogeneous membrane the curvature Gibbs free energy is given by

$$G_{curv} = K_{bend}\left(\frac{1}{R}\right)^2 \qquad , \tag{7}$$

where the bending modulus, K_{bend}, is a function of temperature. It is related to the heat capacity as follows:

$$K_{bend}^{-1} = f \cdot \frac{1}{K_{bend}^{fluid}} + (1-f) \cdot \frac{1}{K_{bend}^{gel}} + \frac{16\gamma_{area}^2\, T}{D^2\, A}\Delta c_P \qquad , \tag{8}$$

where f is the fraction of fluid lipid, K_{gel} and K_{fluid} are the bending moduli of the pure gel or fluid phases, respectively, A is the membrane area and D is the membrane thickness [23]. The bending modulus, as predicted from Eq.8 and the experimental heat capacity profile of DPPC unilamellar vesicles are shown in Fig. 7. The symbols are measurements of the bending modulus as obtained from an optical trapping method [28, 27]. The good agreement between prediction and experiment justifies the above assumption that $\Delta A(T) \propto \Delta H(T)$.

3.3 Relaxation times

When a lipid membrane is perturbed by an external change in pressure or temperature, it relaxes into the new equilibrium state within a period of time called the relaxation time. The system is driven back to equilibrium by the thermodynamic forces, which represent a concept from non-equilibrium thermodynamics. It can be demonstrated that the fluctuations shown in Fig.7 can be used to calculate these forces [31]. Essentially it can be concluded that the relaxation times close to the

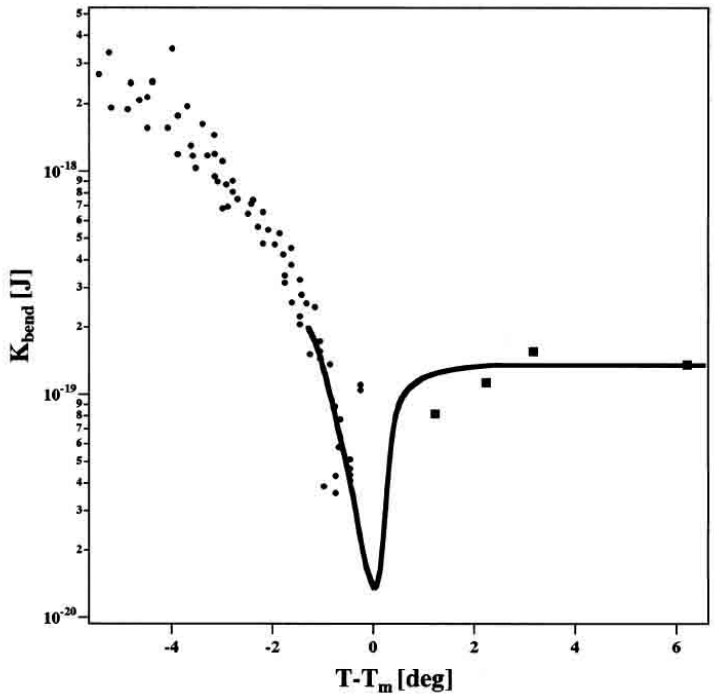

Figure 7: Temperature dependence of the bending rigidity as estimated from the heat capacity of unilamellar DPPC vesicles (solid line) [23] and as measured for unilamellar DMPC vesicles (symbols) [27, 28, 29, 30]. The membranes are more flexible by about one order of magnitude in the melting transition regime.

melting transition are proportional to the heat capacity

$$\tau = \frac{R\,T^3}{L} \cdot \Delta c_p \tag{9}$$

where $L \approx 2 \cdot 10^{12} J^2 K/mol^2 s$.

3.4 Summary response functions

In summary it must be stated that membranes become very flexible close to the melting transition in a simple relation with the heat capacity changes. Thus, for all lipid systems (single lipids, lipid mixtures, biological membranes) showing melting events, the changes in the elastic constants can be predicted from heat capacities. If structural changes of membrane assemblies are possible - e.g. changes in vesicular shape or in membrane topology, they will be most likely to occur in the chain melting regime. Since large fluctuations are also equivalent to the relaxation times, equilibration to a new state will be slow when the elastic constants (and the heat capacity) are large.

4. CHANGES IN STRUCTURE AND TOPOLOGY

The large change in the elastic constants close to the melting transition gives rise to structural changes, because the free energy of bending becomes small. However, the bending free energy is still positive and requires a driving force to favor different geometries. One possible factor in the determination of membrane structure is its interaction with the solvent. Another possibility is the interaction with other molecules or surfaces.

4.1 General considerations

Let us now consider a membrane patch which undergoes a transition between two different geometries. It has been shown both, theoretically and experimentally [32, 18] that curvature broadens the melting transition, meaning that the heat capacity profiles of curved membranes are different from those with a flat geometry. That heat capacities should change can be understood intuitively by looking at

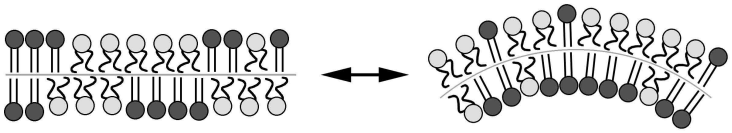

Figure 8: Equilibrium between a flat and a curved membrane patch. The curvature leads to a rearrangement of gel and fluid lipids on the two monolayers.

Fig.8. This figure shows the equilibrium between a flat and a curved geometry at the melting point (equal number of gel and fluid lipids). However, for the curved geometry the number of fluid lipids on the outer monolayer must be larger than on the inside, because gel and fluid lipids possess different areas. The flat geometry has equal numbers of gel and fluid lipids on both sides. Thus, the number of ways in which gel and fluid lipids can be arranged on both monolayers is different in the two cases, and the entropy of the two configurations is different, even though the total number of fluid lipids is identical for flat and curved geometry. Using statistical thermodynamics models the broadening of the heat capacity profile induced by a well defined curvature change can be calculated [18]. The free energy of a membrane with respect to the gel state is given by

$$G(T) = G_0 + \underbrace{\int_{T_0}^{T} \Delta c_P dT}_{H} - T \underbrace{\int_{T_0}^{T} \frac{\Delta c_P}{T} dT}_{S} \tag{10}$$

with G_0 being a term describing the interaction of the membrane with the environment. From the changes in heat capacity the elastic free energy change can be

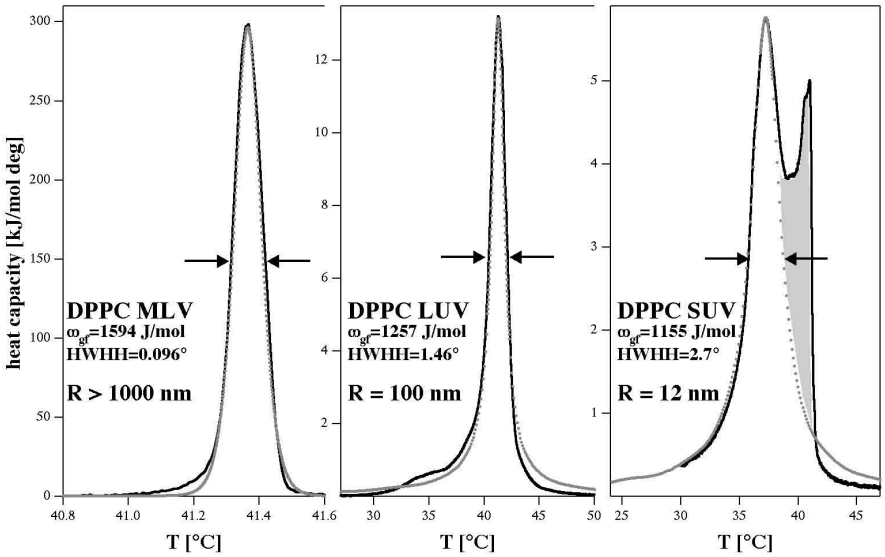

Figure 9: The effect of curvature on the heat capacity profiles: three different vesicular preparations of DPPC with different mean curvature are shown. Left: Multilamellar vesicles with a nearly flat surface. Center: Larger unilamellar vesicles with $R \approx 100nm$. Right: Small unilamellar vesicles from ultrasonication with $R \approx 12nm$ (the shaded area represents a remaining fraction of large vesicles). Solid lines represent experimental profiles, dotted lines are simulated profiles from Monte Carlo simulations [18].

calculated via

$$\Delta G_{elast}(T) = \underbrace{\int_{T_0}^{T} (\Delta c_P^{curved} - \Delta c_P^{flat}) dT}_{\Delta H_{elast}} - T \underbrace{\int_{T_0}^{T} \frac{(\Delta c_P^{curved} - \Delta c_P^{flat})}{T} dT}_{\Delta S_{elast}} \qquad (11)$$

The total free energy change between a flat and a curved membrane segment is the sum of the elastic component and the interaction with the environment, which includes interactions with solvent, membrane associated proteins or surfaces. None of these terms depend on the melting process and they are collectively described by ΔG_0.

$$\Delta G(T) = \Delta G_0 + \Delta G_{elast} \qquad (12)$$

Defining $K = \exp(-\Delta G(T)/RT)$, the free energy of the membrane patch is given by

$$G_{membrane}(T) = G_{flat}(T) \cdot \frac{1}{1+K} + G_{curved}(T) \cdot \frac{K}{1+K} \qquad , \qquad (13)$$

where G_{flat} and G_{curved} have been obtain from heat capacity profiles of flat and curved membranes using Fig. 9 and Eq.10. The heat capacity profile of a system in which equilibrium between flat and curved membrane segments is allowed can

be calculated from Eq.13 using the relation $c_P = -T(\partial^2 G/\partial T^2)_P$. The elastic free energy term in Eqs.11 and 12 is generally positive for a symmetric membrane (Fig.10, left upper panel). If G_0 is zero, the equilibrium constant, K, between the two geometries (flat and curved) is small at all temperatures and the heat capacity of the membrane system is nearly identical to the of a flat membrane (Fig.10, left bottom panel). If, however, G_0 is sufficiently negative, the free energy $\Delta G(T)$ can become negative close to the melting transition (Fig.10, right upper panel). Thus, the equilibrium constant, K, may become larger than unity close to the melting transition and the membrane can then undergo a transition from a flat to a curved geometry. The heat capacity profile, calculated from Eq.13 now displays three peaks (Fig.10, right bottom panel). The left peak represents the structural transition from flat to curved, the right peak represents the transition from curved to flat and the center peak is the melting peak of the curved membrane. This splitting of the heat capacity profile only occurs if G_0 is negative, meaning that the interaction of the curved membrane segment with the environment is more favorable than the interaction of the flat segment with the environment.
Outside of the transition regime the flat geometry will prevail, because the bending elasticity is low and the free energy required to bend the membrane is high.

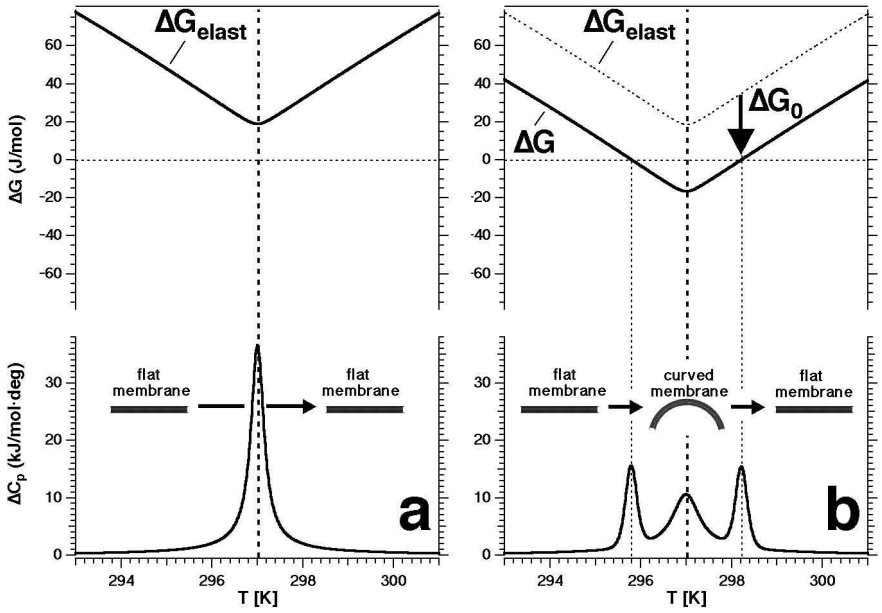

Figure 10: Left: Assuming two states of a membrane patch, one flat and the other curved, one can calculate the bending free energy difference ΔG_{elast} from the heat capacity profiles (top). If $\Delta G_{elast} > 0$, the flat geometry is thermodynamically stable. Right: If the free energy difference between flat and curved is shifted to lower values due to a different interaction of both conformations with the aqueous medium, ΔG can change its sign (top). Under these conditions conformational changes and the heat capacity profile splits into a pattern with three maxima, corresponding to the geometrical changes and the melting of the curved phase (bottom).

Within the transition regime, however, the membrane is very soft and can adapt to the most favorable interaction with the environment.

The theoretical considerations are of course based on some very simplifying thoughts. However, there are several experimental systems that exactly behave in this way. The splitting of heat capacity profiles into several peaks indicates the existence of a coupling of the melting transition with changes in membrane geometry. As examples, we will show in the next sections the transitions of anionic system from vesicles to extended membrane networks, and ripple phase formation. Both examples fit into the above pattern.

4.2 Membrane networks

The anionic lipid dimyristoyl phosphatylglycerol (DMPG) is a negatively charged lipid. It has been observed that this lipid at low ionic strength displays a rather peculiar behavior [33, 34, 35, 36, 37]. The basic features of the melting process are shown in Fig.11a. DMPG dispersions display a heat capacity profile which extends over a wide temperature regime. The integrated heat yields the heat of melting expected for this lipid. Thus, the profile represents a melting process which extends over a broad range of temperatures [33]. The profile shows three distinct peaks, one at the onset of the profile, on in the center and one at the upper end of the transition. Simultaneously, the viscosity of the lipid dispersion increases considerably between the two outer peaks (Fig.11a, center trace), and the dynamic light scattering intensity is reduced [33, 34], indicating a change in the geometry of the membrane assembly [36]. A detailed analysis (using negative stain electron microscopy, freeze fracture electron microscopy and cryo transmission electron microscopy) reveals a microscopic picture of the chain of events [33, 36] (Fig.11a, top): Below the heat capacity events the lipid dispersion exists as a dispersion of large vesicles, which undergo a structural change to a long range membrane network upon shifting the temperature to within the melting regime. Above the melting regime a dispersion with vesicles was found, with vesicle sizes much smaller than in the gel phase. From this it can be concluded that the vesicles in the gel phase have fused into a long range membrane network. Further heating to temperatures above the melting events resulted in spontaneous formation of vesicles. All of these events are fully reversible upon heating and cooling.

The splitting of the heat capacity profile is dependent on the interaction with the solvent. Increasing the lipid concentration [33], addition of polyethyleneglycol and increase of the ionic strength [36] reduce the temperature range of the calorimetric events. Since at low ionic strength electrostatic interactions are long ranged, we take these findings as a proof for that the free energy contribution, ΔG, which describes the interaction with solvent (or environment), favors the

long range network. Reducing the water content or increasing the ionic strength reduces the favorable interaction with solvent.

Obviously the formation of long range networks is a consequence of the long

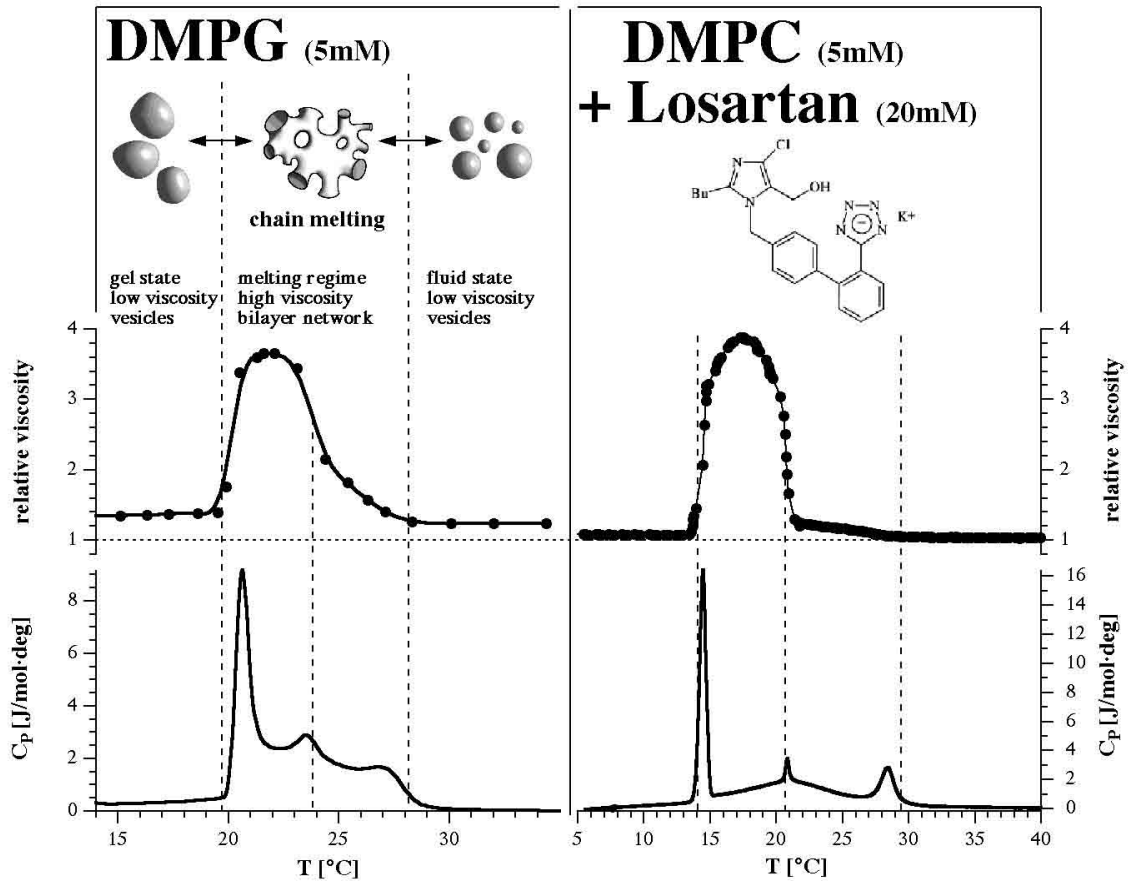

Figure 11: Left: Experimental heat capacity profile of a dispersion of the anionic lipid DMPG at 20mM ionic strength (bottom) and the increase in viscosity in the phase transition regime (center). The heat capacity profile is very similar to that calculated in Fig.10. The increase in viscosity indicates changes in the long range geometry of the lipid membranes. The chain of events is a transition from large unilamellar vesicles to bilayer networks back to smaller unilamellar vesicles upon temperature increase (top). Right: In zwitterionic membranes on can induce similar heat capacity profiles when adding Losartan to the membranes. The viscosity again increases in the melting regime. Thus, external charging of neutral membranes can lead to a coupling of chain melting and membrane structural changes.

range electrostatic contribution of the charged membranes. Interestingly, one can charge membranes with small drugs. The pharmaceutical company Merck distributes a drug called Losartan^{TM} against high blood pressure, which acts as an angiotensin receptor antagonist. Since this drug is rich in aromatic groups it binds to the head group region of zwitterionic membranes. Losartan carries one net negative charge and can thus be considered as an agent that charges the surface. The heat capacity profiles of DMPC in the presence of Losartan looks surprisingly

similar to the heat capacity profiles of DMPG dispersions [38]. Fig. 11 (right) shows the heat capacity trace of a 5mM dispersion of extruded unilamellar vesicles in the presence of 20mM Losartan and the corresponding viscosity profiles. Furthermore, in the melting regime the dynamic light scattering amplitude is reduced and the viscosity is increased, indicating structural changes very similar to those occurring in DMPG dispersions.
It seems likely that the charging of membranes generally promotes structural changes close to the chain melting transition. In our group we have further investigated DMPC at low pH (protonation of the phosphates), and phoshpatidylglycerols with different chain lengths and modified head groups (unpublished data). All of these lipids displayed structural changes close to the melting points. Thus, structural changes close to melting events seem to be a general phenomenon.

4.3 The pretransition

The pretransition is a low enthalpy transition found in many lipid systems below the main chain melting transition. Above the pretransition and below the main chain melting transition the membrane surface adopts a pattern of periodic ripples. This phase has therefore been called the ripple phase (or P'_β-phase, see Fig.12). In the literature the pretransition is commonly considered as an event indepen-

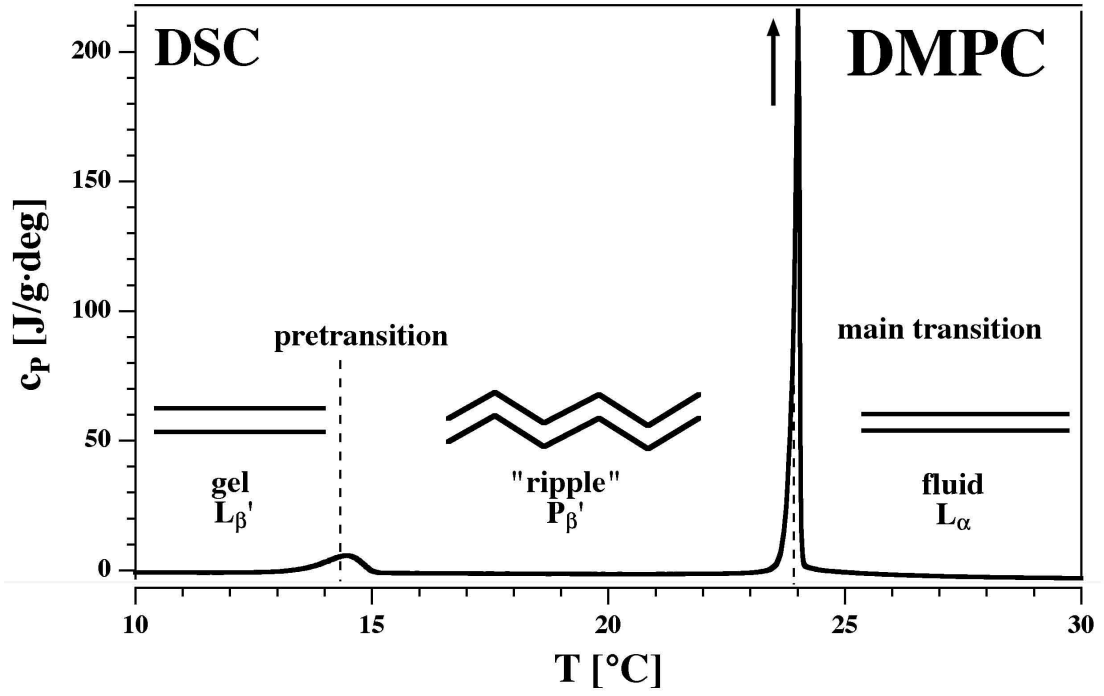

Figure 12: Heat capacity profile of DMPC multilamellar membranes, showing pre- and main transition. In between the two transitions the membrane adopts a different geometry, the so-called ripple phase, which displays periodic surface undulations with periodicities of about 10-20 nm. Above the main transition and below the pretransition the membrane is flat.

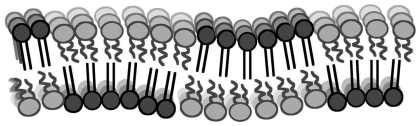

Figure 13: Ripple phase formation by antisymmetric, periodic fluid domain formation (black: gel lipids, white: fluid lipids).

dent from chain melting, caused by tilting of lipid chains and undulations in lipid position, and various models exist in the literature based on purely geometrical arguments. This line of thought, however, seems to be unplausible considering the following experimental findings: During the chain melting transition both enthalpy and volume change, and so do surface area and the chain order parameter (as determined from electron spin resonance [39, 31]). All these system properties also change in the pretransition. Furthermore, the ratio between enthalpy and volume change, as well as the ratio between change in order parameter and enthalpy, display very similar values in both, the main and the pretransition [31]. Since all physical events in the pre- and the main transition are very similar, it is likely that both transitions are caused by a similar physical phenomenon, namely chain melting. In fact, the pretransition may be a phenomenon very similar to the formation of extended bilayer networks in so far as it is also a structural transition linked to a chain melting transition.

One may thus assume that ripple formation takes place via the formation of a periodic pattern of fluid chains arranged along the principle axes of the hexagonal array of lipids (Fig.13, see also Fig.8). Such a behavior would automatically explain the enthalpy, volume, area and order changes in the transition regime, but also the observation that membrane ripple displays typically 120°-angles. Such assumptions have been implemented in a Monte-Carlo simulation [31], assuming that fluids domains on one side and gel domains on the other side result in a local curvature. The periodic arrangement of fluid and gel domains in such a calculation is stabilized by the fact that in multilayers or vesicles with fixed ratios of the areas of outer and inner monolayers, the number of fluid domains on both sides must be equal. Furthermore, it is known that the ripple phase is stabilized by hydration (as is the membrane network in the previous paragraph), and therefore the locally curved regions are favorable if the elasticity of the membranes is large as is the case close to the melting transition. Fig.14 shows the result of such a simulation. The heat capacity profile splits into two peaks due to the coupling with the change in geometry caused by the ripple formation. On the right hand side of Fig.14 some representative Monte Carlo snapshots show how the periodic ripples occur in between the pre and the main transition, whereas the membrane is nearly flat outside of this temperature regime.

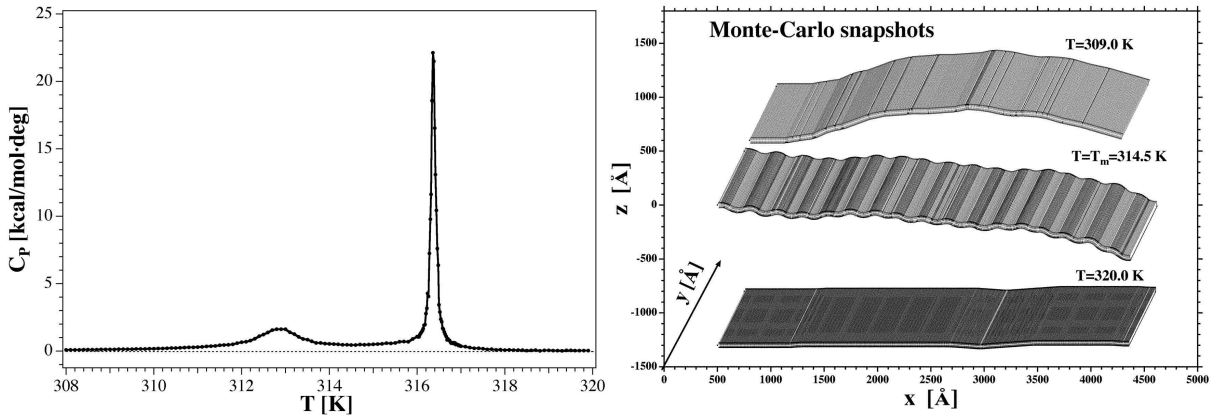

Figure 14: Left: Heat capacity profile of a simulated DPPC bilayer showing pre- and main transition. Right: Monte Carlo snapshots of membranes below the pretransition (top), in the ripple phase regime (center), and above the main transition (bottom). Adapted from [31].

4.4 Summary

Summarizing it must be stated that in general geometric transitions in vesicular structure become more likely close to the chain melting transition. If structural transitions occur in this temperature regime, they lead to a splitting of the heat capacity profile into several maxima which can be attributed to the structural changes and the melting of the intermediate phase. Thus, chain melting and structural transitions are coupled events which are likely to be quite common phenomena. If structural transitions are not taken into account, the interpretation of heat capacity profiles can be quite misleading.

The next chapter will focus on how proteins may influence the fluctuations and thus the elastic constants.

5. HEAT CAPACITY CHANGES INDUCED BY PROTEINS

The interaction of peptides with lipids can also be described using simple statistical thermodynamics models [17, 40, 18]. As in the lipid mixtures, the models are based on relatively few parameters: The melting enthalpy and entropy of the lipid system, and three nearest neighbor interaction parameters, describing the interfacial energy between gel and fluid lipids, between gel lipid and peptide, and between fluid lipid and peptide. These parameters can be obtained from experiment by fitting experimental heat capacity profiles. Some simple cases of peptide mixtures with lipid membranes were discussed by Ivanova et al. [18]. It can be shown that the influence of peptides on the c_P-profiles is mainly due to the mis-

cibility of the peptide with the two lipid phases, gel and fluid, respectively. If,

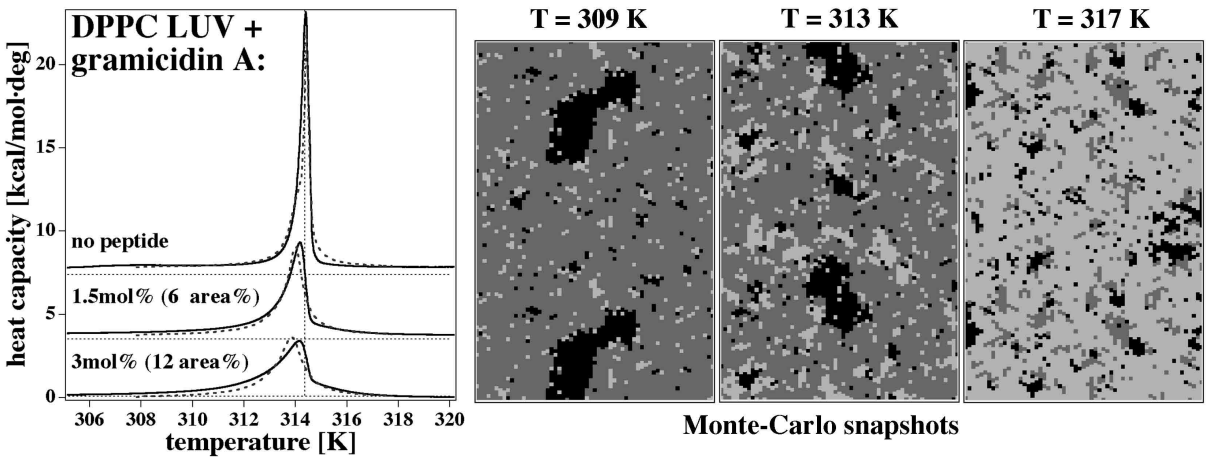

Figure 15: Interaction of gramicidin A with DPPC membranes. Left: heat capacity profiles of DPPC membranes containing 0, 1.5 and 3 mol% of gramicidin A. Solid lines: calorimetric experiments, dashed lines: Monte-Carlo simulations. Right: Monte-Carlo snapshots of the lipid/peptide-matrix from simulations at three different temperatures. The peptide (black dots) tends to aggregate in both, gel (dark grey dots) and fluid (light gray dots) phase. The aggregates in the fluid phase are smaller.

for instance, the peptide mixes well with the fluid phase (low nearest neighbor interaction energy) and does not mix well with the gel phase (high nearest neighbor interaction energy), the peptide would homogeneously distribute in the fluid phase but aggregate in the gel state. The corresponding heat capacity profile will be shifted to lower temperatures and display an asymmetric broadening at the low temperature side of the transition [18]. As an example we can take the interaction of gramicidin A with DPPC large unilamellar vesicles (LUV).
Fig.15 (left hand panel) shows the heat capacity profiles of DPPC LUVs with various concentrations of gramicidin A. It can be seen that the peptide leads to a slight shift of the c_p-profile to lower temperatures, and to an asymmetric broadening at the low temperature end. However, the influence on the heat capacity profiles is not very pronounced. One may conclude from this that the peptide interacts better with the fluid phase than with the gel phase, but tends to form aggregates or clusters in both phases. The Monte Carlo snapshots obtained during the simulation of the heat capacity profiles are shown on the right hand side of Fig.15. Peptides are shown as black dots, and the tendency to aggregate into clusters can well be seen in this simulation. This finding predicts the behavior of gramicidin A in real membranes and we have shown by atomic force microscopy that gramicidin A indeed aggregates in both lipid phases (Ivanova et al., submitted 2002).
In order to fully understand the physical behavior of lipid/peptide systems, it is important to investigate the effect of fluctuations in state (see above). Since the lipid/peptide matrix is not homogeneous, the fluctuations are also different at dif-

ferent locations of the matrix. To calculate such local fluctuations, we proceeded as follows: The lipid/peptide mixture was simulated with the parameters necessary to describe the experimental heat capacity profile. Usually the Monte-Carlo simulation was performed over several thousand cycles to equilibrate the system, including steps to switch the lipid state between gel and fluid state, and steps to let the peptides diffuse. Now we switch the diffusion off, and average the lipid state and derive the fluctuation in state for each lipid site. The fluctuations of the system already shown as snapshots in Fig.15 can be seen in Fig.16 for three temperatures, two of which are below the melting point of the pure lipid (314.3K) and one above the melting point. The height profiles correspond to the fluctuation strength. It can be seen that the fluctuations in the pure lipid matrix at all three temperatures are small, whereas in the peptide containing system the fluctuations are significantly altered. They are especially high close to the peptides.

Taking into account that high fluctuations are equivalent to flexible membranes

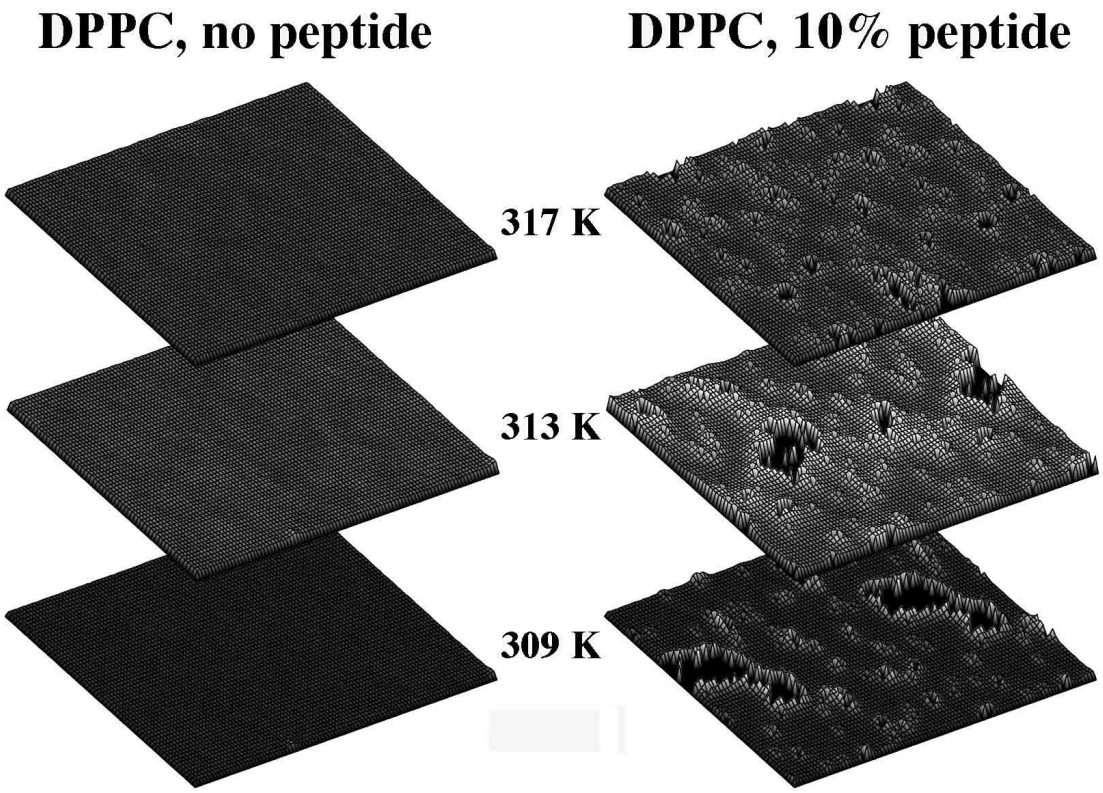

Figure 16: Local lipid fluctuations in a membrane without gramicidin A (left) and containing 10 mol% gramicidin A (right) at three different temperatures below and above the melting point of the lipid (314.3 K). The fluctuations of the lipid matrix in the absence of peptides are small and homogeneous at all given temperatures, but depending on temperature, the fluctuations in state are altered by peptides and can be significantly enhanced close to the gramicidin aggregates (black regions).

with slow relaxation rates, one has to conclude that proteins are able to alter the

mechanical properties and the response times in the direct environment. It is very likely that nature will make use of this mechanism to control the elastic constants of the environment and its relaxation behavior. It has been estimated by Grabitz et al. [41] that in biological membrane relaxation times in the range from 1-10ms can be expected, which roughly corresponds to many enzymatic turnover rates and to opening times of membrane ion channels. Furthermore, since fusion of bilayers requires local curvature, proteins may locally induce fluctuations that facilitate membrane fusion.

6. STRUCTURAL CHANGES IN BIOLOGY

Structural changes in biology are quite important, for example in secretion or in synaptic fusion and fission, or endo- and exocytosis, respectively [42, 43] (Fig.17). Endocytosis is thought to be the key process by which the nerve pulse gets across

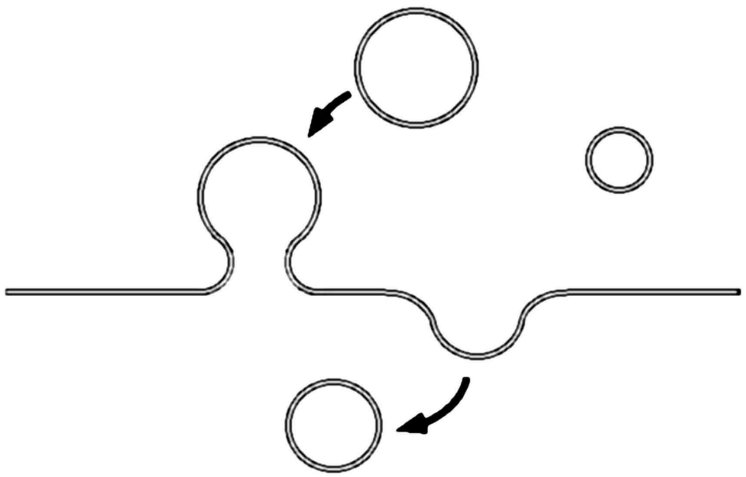

Figure 17: Schematic drawing of fusion and fission events in membranes, as they occur in endocytosis and exocytosis.

the synaptic cleft. The synapse contains a large number of vesicles of about 100nm in diameter. They contain various neurotransmitters, which are mostly small aromatic molecules that partition quite well into the head group region of lipid membranes. Endocytosis involves the fusion of synaptic vesicles with the presynaptic membrane. After the fusion initiation, neurotransmitters are released into the synaptic cleft, where they trigger an excitation of the postsynaptic membrane. In detail, the endocytosis is assumed to be initiated by calcium influx into the synapse, where the calcium interacts with a group of proteins called the snare proteins. These proteins are thought to undergo a conformational change, which then causes the fusion of synaptic vesicles with the presynaptic membrane. In

these models, the main event in the fusion is the formation and a subsequent conformational change of the snare complex [42, 43]. Thus, it represents a model on a single molecular basis.

In contrast, the view of synaptic fusion by a certain theoretical physicists school is purely based on macroscopic elasticity theory. The theoretical concepts of membrane elasticity, introduced by Helfrich [44], have been used by various authors to describe fusion intermediates on the basis of local curvature [45, 46]. In these models proteins or individual molecules don't play a defined role. The elastic constants are assumed to be constant throughout the whole membrane of both, synaptic vesicle and presynaptic membrane. Therefore, the molecular biology vision and the theoretical physicists calculations are based on very different assumptions and concepts. None of these models make any use of heterogeneities in the membrane or fluctuations.

It seems to be a fact that snare proteins are involved in the fusion process. Furthermore, synaptic membranes are not homogeneous but contain cholesterol rich domains, where snare proteins are colocalized. When cholesterol is removed, synaptic fusion is inhibited [47]. Thus, it is also very probable that the concepts of fluctuations, closely linked to domain formation and protein clustering, will contribute to the physics of membrane fusion in synapses. Fluctuations are the physical way to make a system adaptable to changes in the environment, may they be changes in calcium concentration, protein binding, pH changes or sudden changes in temperature.

7. SUMMARY

In this contribution we have outlined how chain melting events are linked to changes of the elastic constants, based on a theory for the fluctuations of lipid membranes. Using these concepts we were able to explain several known examples of structural changes of membranes systems, including to reversible fission and fusion of anionic lipid vesicles and the formation of the ripple phase. Fluctuations were also shown to be the basis for domain formation. They are strongly influenced by temperature, but also by pH changes and calcium. The presence of proteins can locally change the membrane state and thus influence elastic constants, relaxation times and domain formation. Additional to the high chemical specificity of individual proteins, these physical and unspecific mechanisms provide a powerful mechanism for the control of biological function.

Acknowledgments
I am grateful to Thomas Schlötzer, Heiko Seeger and Denis Pollakowski from the ‘Biophysics and Thermodynamics of Membranes Group’ to let me use some of their data prior to publication. Lung surfactant was a kind donation of Fred Possmeyer (University of Western Ontario, London, Canada). Martin Zuckermann helped proof-reading the manuscript. TH was supported by the Deutsche Forschungsgemeinschaft (DFG, Grants He1829/6 and He1829/8).

References

[1] G. Cevc and D. Marsh. Phospholipid Bilayers: Physical Principles and Models. Wiley, New York (1989).

[2] R. B. Gennis. Biomembranes. Molecular structure and function. Springer, New York (1989).

[3] E. Neher and B. Sakmann. Nature, 260 (1976) 779.

[4] B. Hille. Ionic channels of excitable membranes. Cambridge University Press, Cambridge (1957).

[5] C. K. Mathews and K. E. van Holde. Biochemistry. The Bejamin/Cummings Publishing Company, Redwood City, Ca (1990).

[6] E. Sackmann. Physical basis of self-organization and function of membranes: Physics of vesicles. in: Structure and Dynamics of Membranes: From Cells to Vesicles. R.Lipowski and E. Sackmann, eds., Elsvier, Amsterdam (1995) 213–304.

[7] J. L. C. M. van de Vossenberg, A. J. M. Driessen, M. S. da Costa and W. N. Konings. Biochim. Biophys. Acta, 1419 (1999) 97.

[8] H. Ebel, P. Grabitz and T. Heimburg. J. Phys. Chem. B, 105 (2001) 7353.

[9] A. G. Lee. Biochim. Biophys. Acta, 472 (1977) 285.

[10] I. P. Sugar, T. E. Thompson and R. L. Biltonen. Biophys. J., 76 (1999) 2099.

[11] K. Simons and E. Ikonen. Nature, 387 (1997) 569.

[12] D. A. Brown and E. London. Ann. Rev. Cell Develop. Biol., 14 (1998) 111.

[13] T. Harder, P. Scheiffele, P. Verkade and K. Simons. J. Cell Biol., 141 (1998) 929.

[14] A. Rietveld and K. Simons. Biochim. Biophys. Acta, 1376 (1998) 467.

[15] M. Bagnat, S. Keranen, A. Shevchenko and K. Simons. Proc. Natl. Acad. Sci. USA, 97 (2000) 3254.

[16] J. H. Ipsen, O. G. Mouritsen and M. J. Zuckermann. Biophys. J., 56 (1989) 661.

[17] T. Heimburg and R. L. Biltonen. Biophys. J., 70 (1996) 84.

[18] V. P. Ivanova and T. Heimburg. Phys. Rev. E, 63 (2001) 1914.

[19] O. G. Mouritsen, M. M. Sperotto, J. Risbo, Z. Zhang and M. J. Zuckermann. Computational approach to lipid-protein interactions in membranes. in: Advances in Computational Biology. H.O. Villar, ed., JAI Press, Greenwich, Conneticut (1995) 15–64.

[20] O. G. Mouritsen and K. Jorgensen. Mol. Membr. Biol., 12 (1995) 15.

[21] L. Cruzeiro-Hansson, J. H.Ipsen and O. G. Mouritsen. Biochim. Biophys. Acta, 979 (1990) 166.

[22] M. Nielsen, L. Miao, J. H. Ipsen, M. J. Zuckermann and O. G. Mouritsen. Phys. Rev. E, 59 (1999) 5790.

[23] T. Heimburg. Biochim. Biophys. Acta, 1415 (1998) 147.

[24] S. Halstenberg, T. Heimburg, T. Hianik, U. Kaatze and R. Krivanek. Biophys. J., 75 (1998) 264.

[25] W. Schrader, H. Ebel, P. Grabitz, E. Hanke, T. Heimburg, M. Hoeckel, M. Kahle, F. Wente and U. Kaatze. J. Phys. Chem. B, (2002). In press.

[26] E. A. Evans. Biophys. J., 14 (1974) 923.

[27] T. Heimburg. Curr. Opin. Colloid Interface Sci., 5 (2000) 224.

[28] R. Dimova, B. Pouligny and C. Dietrich. Biophys. J., 79 (2000) 340.

[29] L. Fernandez-Puente, I. Bivas, M. D. Mitov and P.Meleard. Europhys. Lett., 28 (1994) 181.

[30] P. Meleard, C. Gerbeaud, T. Pott, L. Fernandez-Puente, I. Bivas, M. D. Mitov, J. Dufourcq and P. Bothorel. Biophys. J., 72 (1997) 2616.

[31] T. Heimburg. Biophys. J., 78 (2000) 1154.

[32] T. Brumm, K. Jorgensen, O. G. Mouritsen and T. M. Bayerl. Biophys. J., 70 (1996) 1373.

[33] T. Heimburg and R. L. Biltonen. Biochemistry, 33 (1994) 9477.

[34] K. A. Riske, M. J. Politi, W. F. Reed and M. T. Lamy-Freund. Chem. Phys. Lett., 89 (1997) 31.

[35] K. A. Riske, O. R. Nascimento, M. Peric, B. L. Bales and M. T. Lamy-Freund. Biochim. Biophys. Acta, 1418 (1997) 133.

[36] M. F. Schneider, D. Marsh, W. Jahn, B. Kloesgen and T. Heimburg. Proc. Natl. Acad. Sci. USA, 96 (1999) 14312.

[37] K. A. Riske, H.-G. Döbereiner and M. T. Lamy-Freund. J. Phys. Chem. B, 106 (2002) 239.

[38] E. Theodoropoulou and D. Marsh. Biochim. Biophys. Acta, 1461 (1999) 135.

[39] T. Heimburg, U. Würz and D. Marsh. Biophys. J., 63 (1992) 1369.

[40] T. Heimburg and D. Marsh. Thermodynamics of the interaction of proteins with lipid membranes, Birkhäuser, Boston (1996) 405–462.

[41] P. Grabitz, V. P. Ivanova and T. Heimburg. Biophys. J., 82 (2002) 299.

[42] R. Jahn and T. C. Südhof. Ann. Rev. Neurosci., 17 (1994) 219.

[43] R. Jahn and T. C. Südhof. Ann. Rev. Biochem., 68 (1999) 863.

[44] W. Helfrich. Z. Naturforsch., 28c (1973) 693.

[45] Y. Kozlovsky and M. M. Kozlov. Biophys. J., 82 (2002) 882.

[46] V. S. Markin and J. P. Albanesi. Biophys. J., 82 (2002) 693.

[47] T. Lang, D. Bruns, D. Wenzel, D. Riedel, P. Holroyd, C. Thiele and R. Jahn. EMBO J., 20 (2001) 2202.